Knowledge-Based Systems 267 (2023) 110413

Contents lists available at ScienceDirect

Knowledge-Based Systems

journal homepage: www.elsevier.com/locate/knosys

Explainable quantum clustering method to model medical data

Shradha Deshmukh [a], Bikash K. Behera [b], Preeti Mulay [a], Emad A. Ahmed [c], Saif Al-Kuwari [d], Prayag Tiwari [e,*], Ahmed Farouk [f,*]

[a] Symbiosis Institute of Technology, Symbiosis International (Deemed University), Pune, India
[b] Bikash's Quantum (OPC) Pvt. Ltd., Mohanpur, WB, 741246, India
[c] Department of Computer Science, Faculty of Computers and Information, South Valley University, Qena, Egypt
[d] College of Science and Engineering, Hamad Bin Khalifa University, Qatar Foundation, Doha, Qatar
[e] School of Information Technology, Halmstad University, Sweden
[f] Department of Computer Science, Faculty of Computers and Artificial Intelligence, South Valley University, Hurghada, Egypt

ARTICLE INFO

Article history:
Received 4 September 2022
Received in revised form 20 January 2023
Accepted 18 February 2023
Available online 23 February 2023

Dataset link: https://github.com/shradha-deshmukh/Explainable-Quantum-Clustering.git

Keywords:
Quantum clustering
Quantum machine learning
Quantum computing
qk-means algorithm
Explainable AI
LIME

ABSTRACT

Medical experts are often skeptical of data-driven models due to the lack of their explainability. Several experimental studies commence with wide-ranging unsupervised learning and precisely with clustering to obtain existing patterns without prior knowledge of newly acquired data. Explainable Artificial Intelligence (XAI) increases the trust between virtual assistance by Machine Learning models and medical experts. Awareness about how data is analyzed and what factors are considered during the decision-making process can be confidently answered with the help of XAI. In this paper, we introduce an improved hybrid classical-quantum clustering (improved qk-means algorithm) approach with the additional explainable method. The proposed model uses learning strategies such as the Local Interpretable Model-agnostic Explanations (LIME) method and improved quantum k-means (*qk*-means) algorithm to diagnose abnormal activities based on breast cancer images and Knee Magnetic Resonance Imaging (MRI) datasets to generate an explanation of the predictions. Compared with existing algorithms, the clustering accuracy of the generated clusters increases trust in the model-generated explanations. In practice, the experiment uses 600 breast cancer (BC) patient records with seven features and 510 knee MRI records with five features. The result shows that the improved hybrid approach outperforms the classical one in the BC and Knee MRI datasets.

1. Introduction

Artificial Intelligence (AI) has achieved widespread success in various fields. A tremendous amount of data is generated daily to monitor routine tasks or help humans to improve their life. Deep learning is a significant factor in developing knowledgeable learning from the generated data. Managing complex data containing numerous features is increasingly time-consuming. Hence, models are very often used as black boxes that process input data and output predictions or decisions. This black box approach leads to non-transparent models and it can not be explained how the conclusions or predictions are made. The black box characteristics create problems while presenting predictions or making decisions. These decisions must have some explanations which show the transparent method of predictions. In the endeavor to address non-transparency, Explainable AI (XAI) comes into the picture and is also known as interpretable machine learning (ML) [1]. Several explainable and interpretable methods have been proposed in recent years. A model-based or post-hoc method is discussed and used in [2]. For instance, CT scan data is fed to the trained AI model for explainable prediction of lung cancer, presented in [3]. The XAI helps to determine why a particular CT scan was classified as lung cancer. XAI also explains how the model works and what factors are important in an overall manner. XAI methods focus on global and local explainability to see the relevant features and the decision probability.

1.1. Categorization in explainable AI

XAI is an add-on option when using ML algorithms to generate human understandable decisions [4], but it is rapidly gaining popularity in many applications [5–8]. A lot of techniques have been created for supervised algorithms, but since clustering cannot identify the causes of cluster formation, less work has been done to explain unsupervised procedures. Finding the inherent

* Corresponding authors.
E-mail addresses: shradha.deshmukh.phd2020@sitpune.edu.in (S. Deshmukh), bikas.riki@gmail.com (B.K. Behera), preeti.mulay@sitpune.edu.in (P. Mulay), emad.amer@sci.svu.edu.eg (E.A. Ahmed), smalkuwari@hbku.edu.qa (S. Al-Kuwari), prayag.tiwari@ieee.org (P. Tiwari), ahmed.farouk@sci.svu.edu.eg (A. Farouk).

https://doi.org/10.1016/j.knosys.2023.110413
0950-7051/

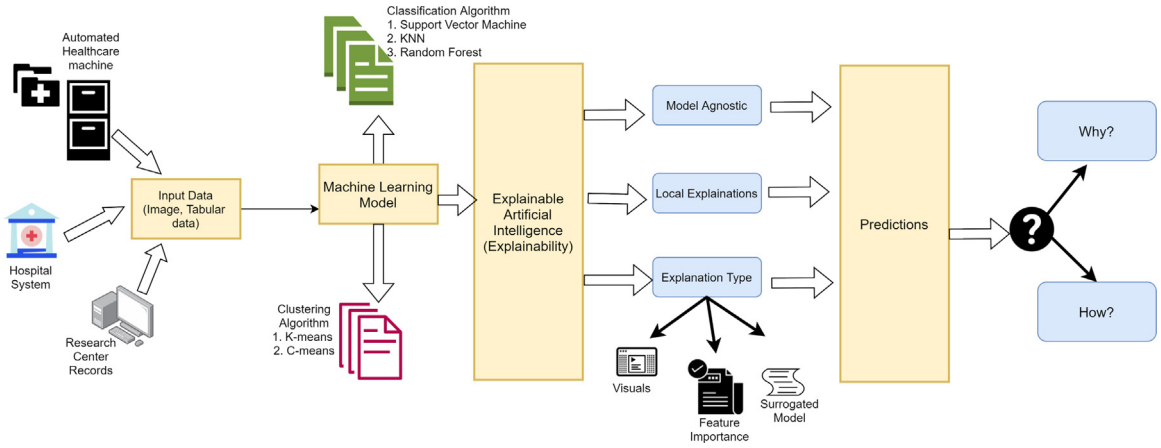

Fig. 1. The overview shows the procedures XAI uses to reach at accurate outcomes produced by the ML model. The input data (all the data types) is accepted in the first stage, after which the appropriate ML model is used to see the outcomes or predictions. The answers to queries like "How and why the predictions are made" are offered by the explanations given by the XAI.

groupings contained within the data is performed using the unsupervised clustering technique. However, it may be challenging to understand why a single row of data is grouped in a certain cluster when clusters are produced using methods like the k-means algorithm. The model can utilize this insight to shift data points from one cluster to a more lucrative cluster by being aware of these boundary constraints for transition from one cluster to another. For decision-makers, explainable clustering is typically advantageous. Some methods can be used to interpret the clustering outcomes of any unsupervised approaches because it is model agnostic [9,10] (which means that these methods can be applied to any model). The classification algorithms like Support Vector Machine (SVM), Random Forest, and K Nearest Neighbor (KNN) are used to categorize the acquired cluster labels and the associated datasets.

Regarding the scope of the provided explanation, we can categorize the methods into global and local approaches. Scope refers to either aiming to explain the whole model or just parts of the model, such as individual predictions. To explain, let us recall that the decision boundary of a complex model can be highly non-linear. For instance, we have a classification problem here, and only a complex function can separate the two classes. Sometimes it cannot explain the global model; instead, many approaches assume a local area. Then we need to explain the individual predictions made at the specified decision boundary. Fig. 1 further differentiates according to the data type a method can handle. A few explainability algorithms can work with all types of data [11]. Finally, the models produce different explanations, starting with correlation plots or other visual methods. Also, obtaining information about the feature's importance is called a feature summary. Other methods return data points that help us understand the model, and some existing approaches build a simple model around the complex one. A simple model, which are usually called surrogates, can then be used to derive explanations. An overview of the XAI model's workflow is shown in Fig. 1, where one of the levels offers the specifics of local explanations, explanation kinds to be examined, and model agnostic categories. The final stage of the XAI model answers the queries of why the model makes a particular prediction and how the prediction is calculated.

In medical or healthcare domain, ML learns from a large amount of data and predicts more accurate results than the average clinicians. With this motivation, the aim is to reduce the accuracy gap while increasing the trust. Sometimes doctors have natural biases, so to overcome this problem, AI produces the objective diagnosis with preconceived socio-economic notions, which ultimately produces trustworthy relations between the parties, such as AI–doctor relations and AI–patient relations.

1.2. Challenges in medical data

There are a number of challenges in the healthcare related to the medical data [12–14], such as:

- Many medical image datasets are unavailable due to privacy concerns.
- Sometimes incorrect labels come up with wrong predictions.
- In some cases, features are strongly correlated, and most training data are uninformative and redundant.
- It is not easy to convert image data into pixel numeric data.

XAI has many challenges and associated issues, as discussed in the context of standard workflow shown in Fig. 2 [15,16]. Designing domain-agnostic systems with XAI is challenging as explanations require the context of rooming. Some explanations can be helpful for the targeted perspective but trivial for others. For instance, presenting interactive visualizations to explain layers of a Neural Network (NN) is beneficial for data scientists but less critical to radiologists who use the NN for data analysis. Integrating XAI in a standard workflow is challenging but it benefits from multiple perspectives [17]. The scope of XAI is broader than the traditional ML model [18]. The explainability of the underlying data and preprocessing methods, such as feature selection utilized for input data preparation, are important issues need to be addressed. Furthermore, if the underlying training data contains records from comparable demographics, the ML models used to forecast a disease based on a patient's medical records may not be acceptable. Another significant obstacle to XAI is its subjective applicability. Healthcare facilities, for instance, have varying degrees of access to medical data in the real world. It is crucial to comprehend, how a single model developed for a certain disease's diagnosis performs in multiple contexts. We suggest a simple and efficient incremental learning method to provide the first steps toward problem-solving and enable a level of explainability based on the recognized collection of linked difficulties.

The feature importance process is shown in Fig. 2 and relates to methods that rate input characteristics according to how well they can predict a target variable. Statistical correlation scores, coefficients derived as part of linear models, decision trees, and permutation importance scores are a few common examples of feature importance scores. At the same time, many other types

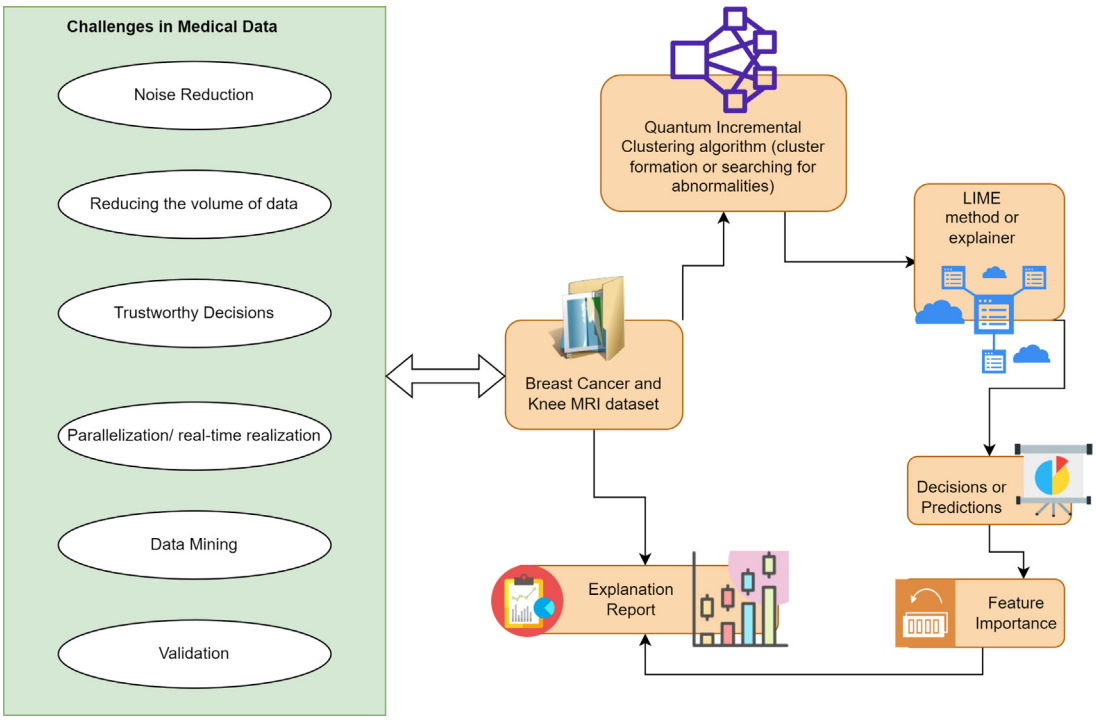

Fig. 2. Overview of the integration of XAI and machine learning models. The data and model come up with high-level explainability of data and then finally show the predictions.

and sources are also discussed in [19]. In predictive modeling, feature importance scores are crucial because they offer insight into the data and the model. Additionally, statistical correlation scores are applied to boost the effectiveness and efficiency of a predictive model. The most popular method for determining if two features are statistically connected is the t-test [20]. The t-test identifies the most important features from the set of features, then the t distribution is used to determine the correct t value, which is in turn used to determine the significance of a correlation coefficient (See Eq. (1)). By assuming no association between them (Sigma= 0), the t value can be computed as follows:

$$t = m\sqrt{\frac{n-2}{1-m^2}} \tag{1}$$

where m is the correlation coefficient for the sample data and n is the total number of data points. Probability levels (p) are used to express the relationship's importance (i.e., the significance at $p = 0.05$). There are n - 2 degrees of freedom when entering the t-distribution. The feature is chosen if the t value exceeds the crucial value at the 0.05 significant level, indicating that it is significant.

Fig. 2 illustrates the proposed steps to deal with the challenges in medical data. The quantum clustering algorithm clusters the data points with matching characteristics, and then the Local Interpretable Model-Agnostic Explanations (LIME) explainer shows the description of the decision or the important feature for the predictions. The detailed report generated from the ML models shows the explanation and maintains the clinical experts' trust.

1.3. Contributions

Our contributions can be summarized as follows:

(1) We propose hybrid approach, i.e. explainability and improved quantum clustering algorithm, for generating the best medical report prediction explanations.
(2) We encode the classical data into quantum states and form the clusters using the improved *qk*-means algorithm, with the help of the $UU^{\dagger}$ quantum circuit.
(3) We show that our proposed model works well in terms of the overall clustering accuracy of the breast cancer and Knee MRI dataset.
(4) We discuss the effectiveness of the improved *qk*-means algorithm with the experimental results obtained from the IBM quantum simulator, i.e. qasm simulator, and show that the hybrid approach outperforms the classical one.
(5) We integrate LIME with the improved *qk*-means algorithm for trustworthy decisions.

1.4. Organization

The rest of this paper is organized as follows: Section 2 highlights the medical literature, how explainability is used to provide expert predictions, and a brief about QML in medical data. Section 3 describes the proposed methodology of the hybrid classical quantum *k*-means algorithm and the implementation of the improved *qk*-means algorithm with LIME. Section 4's experimental result illustrates the evaluation environment, used datasets, and quantitative visualization. The results of explainability and hybrid approach are discussed in Section 5. Finally, Section 6 concludes the paper.

2. Related works

2.1. Explainability in the medical domain

In healthcare, human lives are at stake; therefore, it becomes vital for clinicians to understand the operation of the models and the prediction they make. XAI models help in the following ways:

- Supports in model improvement
- Merge the layer of confidence in the prediction made by the AI models

Furthermore, explanations behind inaccurate predictions can help trace the factors that cause them and improve the model for future use. The medical data field has different applications, such as detection, diagnosis, and treatment plan [21]. XAI assists in diagnosing diseases such as neurology, cancer, and cardiology [22,23]. In the radiology domain, the author explains how to identify the radiographs with a decision to maintain transparency [24]. In the pathology domain, the paper introduces the techniques to recognize the patterns for pathologists to speed up the diagnostic process [25].

Creating the step-wise framework of the ML pipeline process, which includes pre-processing methods, data manipulation, and explainability results, reduces the bias prediction and promotes fairness of the ML model. The pertinent input data from the human records helps to optimize the ML pipeline to obtain effective results to participate in the decision-making process.

2.2. Classical to quantum machine learning in medical data

Technological concerns have dominated the research of ML techniques for medical applications. However, it is crucial to improve the understanding of ML algorithms and to offer mathematical reasoning for their attributes in order to get helpful insight into the performance and behavior of ML approaches in a medical context. The diagnostic accuracy of a patient is traditionally based on a doctor's experience, although this knowledge is gained over many years of observing many patients' symptoms and receiving a verified diagnosis. Even then, accuracy cannot be guaranteed. A large amount of data can now be acquired and stored easily because of the development of computing technologies, as seen in the specialized databases of electronic patient records [26]. By using classification approaches to identify breast cancer patients (differentiate between benign and malignant tumors) to predict prognosis, ML techniques play an important role in the diagnosis and prognosis of breast cancer [15]. The most suitable treatment plan can be prescribed by professionals with the help of accurate classification. Table 2 shows some of the already existing works on the breast cancer dataset. Logistic regression, linear regression, and discriminant analysis are examples of traditional statistical methods for data analysis. To show the benefits of ML and its potential, a number of research works contrasting various classic statistical approaches with classical ML classification methods have been published.

Quantum machine learning (QML) is a new and promising paradigm in the domain of science and technology on today's edge as quantum data science is becoming mainstream [27]. QML fills the gap between theoretical advances in quantum computing and deployed ML science if it focuses on offering synthesis that describes more relevant ML algorithms in a quantum framework reducing the complexity of the disciplines involved. Quantum computing is revolutionalizing the way that we approach ML. This can be achieved by leveraging quantum effects such as entanglement and interference to solve currently unsolvable problems in ML. For example, the quantum kernel method has been shown to be effective as compared to other kernels in the presence of high noise [28]. The hybrid classical-quantum neural network is proposed for healthcare-based intrusion detection systems using quantum circuits [29]. The quantum kernelized binary classifiers are used to simplify the quantum kernel support vector machine and applied to clinical data. The quantum distance classifier technique explains in the literature where authors show the distance calculation using the Hadamard gate and SWAP test [30]. The following formula is used to calculate the distance between two vectors (Eq. (2)). The task is to calculate the $\langle u|v\rangle$ on a quantum computer.

$$|u\rangle - |v\rangle = \det\left||u\rangle|v\rangle\right| - \langle u|v\rangle \tag{2}$$

2.3. Explainability and clustering in medical data

The literature [39] explains multilevel clustering to build explainable data visual mapping. The explained method shows the clustering performed by the external agnostic algorithm on selected parameters to form clusters. With the help of such a method, exploratory information is provided to take knowledge-based actions. The described method successfully explains the accurate labels of the patient report [40]. The literature [41] presents the framework for XAI, that applies the ensemble clustering method to brain injury data. This accommodates the Traumatic Brain data using the ensemble method and presents an effective and an explainable report. Table 1 lists current XAI studies along with specifics on their techniques and targeted datasets.

3. Methodology

3.1. Classical and quantum k-means algorithm

The clustering is an unsupervised learning problem, where input data has no labels and the goal is to form meaningful subgroups with similar features from the data. The classical k-means approach finds the nearest data points of the selected clusters and forms a quality cluster to analyze the unseen data. The classical approach uses the random cluster's centroid, and the radius of the cluster is not defined in the initial phase. The detection of similar featured data points using the Euclidean distance calculation is the standard process used in most literature [42]. The classical approach quickly becomes inefficient when it comes to high-dimensional datasets. The allocation of data points is complex when data carrying the n number of dimensions. The classical-quantum approach uses the quantum clustering method to deal with the n-dimensional data, and provides strong theoretical base to deal with n dimensional data. Here, qk-means algorithm is also called as the hybrid classical-quantum method. Quantum clustering, the distance calculation between the data points and centroids, is exhibited by the probabilistic nature of quantum states. The quantum approach quantifies different probabilities' amplitudes to provide outputs from the classical inputs.

3.2. Dataset: breast cancer and knee MRI datset

In this paper, two different datasets i.e. Breast cancer and Knee MRI are used to discuss the performance of the quantum clustering algorithm.

Systems are increasingly combining relational tabular data with machine learning to intelligently supplement workflows and processes that are typically handled by people. Tabular data is the most frequent data type in business and the second most frequent format in academics, according to a recent poll by the data science platform KAGGLE [43]. For the cluster analysis of tabular datasets, a parallel k-means algorithm implementation that is massively parallel and scalable was created [44]. A logical conjunction of events specifies a generalized representation of patterns, or symbolic object [45]. These events connect values and features to express the data's abstract pattern. According to recent studies, feature extraction continues to put more emphasis on converting the data into a quantifiable data type than it does on identifying fresh patterns to describe the data [46]. In ML, researchers have begun to integrate clustering techniques and classifier models in order to minimize the quantitative training set dimension. A clustering approach is utilized [47,48] to group comparable tabular terms in order to facilitate quicker and more precise training on the job of quantitative data categorization. The fuzzy C-means clustering technique and a K-means version, are

Table 1
XAI methods on medical data.

Sr. no.	Article title	Year	Datasets	Methodology
1.	"ExMed: An AI Tool for Experimenting XAI Techniques on Medical Data Analytics" [31]	2021	Simulacrum Dataset	Explainability for prediction model using the feature attribution model
2.	"Diagnosis support model of cardiomegaly based on CNN using ResNet and explainable feature map" [32]	2021	X-ray dataset	Convolution neural network based ResNet for detection the cardiomegaly diagnosis.
3.	"Explainable Artificial Intelligence for Human Decision Support System in the Medical Domain" [33]	2021	Image data from Video Capsule Endoscopy	Local Interpretable Model-Agnostic Explanations (LIME) and Shapley Additive exPlanations are used to produce the explanations. The output description is evaluated by the professionals.
4.	"Applications of Explainable Artificial Intelligence in Diagnosis and Surgery" [15]	2022	Tomography Image dataset and MRI dataset	Summaries the latest explainability methods applied on Medical data.
5.	"Explainable AI for Glaucoma prediction analysis to understand risk factors in treatment planning" [16]	2022	Coherence tomography eyes image data and clinical data of glaucoma patients	To process data author uses spike neural network (SNN) and adaptive neuro-fuzzy inference systems.

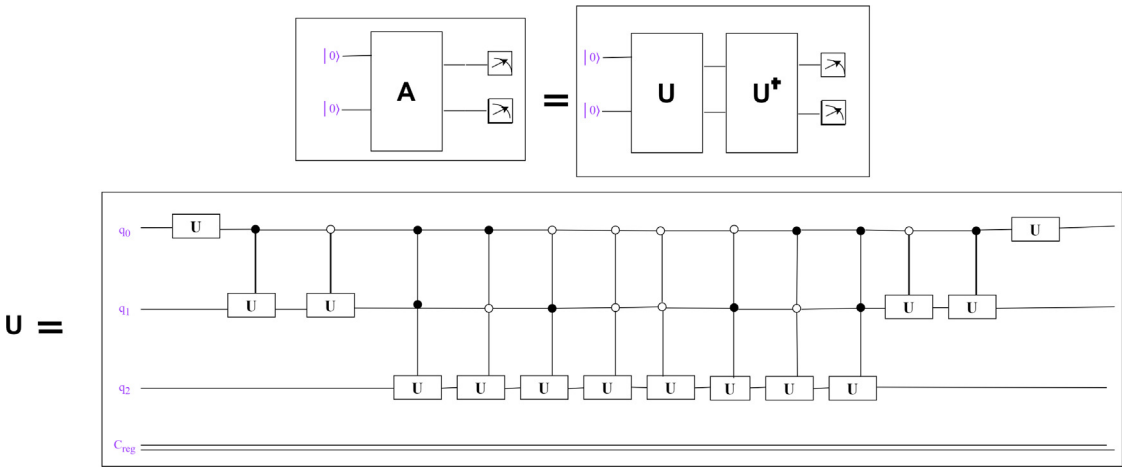

Fig. 3. The quantum circuit for $UU^{\dagger}$ gate for distance calculation in improved *qk*-means clustering algorithm. The circuit is a three-qubit system to show the various features of the input dataset.

Table 2
Performance measure of a classical learning model and classical-quantum learning model on the Breast cancer data (Dataset 1) and Knee MRI data (Dataset 2).

Models and sources	Dataset	Precision	Recall	F1 measure
Classical Classification Algorithms				
KNN [34,35]	Dataset 1	0.904	0.917	0.911
KNN [34,35]	Dataset 2	0.931	0.926	0.915
Random Forest [36]	Dataset 1	0.905	0.917	0.923
Random Forest [36]	Dataset 2	0.908	0.925	0.919
SVM [37]	Dataset 1	0.898	0.885	0.891
SVM [37]	Dataset 2	0.888	0.865	0.832
Logistic Regression [38]	Dataset 1	0.887	0.864	0.891
Logistic Regression [38]	Dataset 2	0.878	0.855	0.889

developed for the SVM classifier training set to explore hidden patterns.

The breast cancer dataset has 600 attributes or patient records and 7 features, whereas the second dataset contains 1370 knee MRI data from Stanford University Medical Center. However, we used 510 Knee MRI data with 5 features for the experiment. Our proposed improved quantum clustering algorithm clusters the MRI data into three cluster labels: anterior cruciate ligament (ACL), meniscal tears, and abnormalities. (Fig. 5).

Encoding Procedure: The basic procedure to encode the classical data points into the quantum states as discussed in [28,49]. The proposed method uses the amplitude encoding technique to encode the selected input data, so the classical data is encoded in quantum state amplitudes.

$$|X\rangle = \sum_{i=2}^{2^n} x_i |i\rangle \tag{3}$$

In Eq. (3), the elements of the amplitude vector are converted into computational basis states. Now the quantum model is integrated with the encoded quantum data and is ready to perform the clustering. Existing literature [50,51] shows that a significant speed-up using the Grover's search algorithm can be obtained, but the quality of clusters is unsatisfactory compared to the classical clustering algorithm.

3.3. Implementation of improved qk-means algorithm

In both datasets, the cluster centroid is allocated, and then the qk-means algorithm is used to find the cluster among them.

Table 3
Results collected from the different clustering metrics are presented for Dataset 1: Breast Cancer dataset, Dataset 2: Knee MRI dataset. In the table, the abbreviations are denoted as, ACC: Accuracy, Com: Completeness, Sils: Silhouette Score.

Models and sources	Dataset	Acc	Com	SilS
Classical Clustering Algorithms				
Classical K-means Algorithm [52]	Dataset 1	0.881	0.872	0.181
Classical K-means Algorithm [52]	Dataset 2	0.873	0.861	0.292
C-means [53]	Dataset 1	0.875	0.861	0.118
C-means [53]	Dataset 2	0.892	0.885	0.221
Classical-Quantum Clustering Algorithms				
qk-means [54]	Dataset 1	0.880	0.897	0.211
qk-means [54]	Dataset 2	0.891	0.881	0.194
Improved *qk*-means (Proposed)	Dataset 1	0.926	0.891	0.333
Improved *qk*-means (Proposed)	Dataset 2	0.937	0.932	0.301

Algorithm 1: Improved *qk*-means algorithm.

Input Classical data
Output Clusters of data
1 Assuming input data points $X_1, X_2, ...X_n$, and k number of clusters, we have $|X_1\rangle, |X_2\rangle, |X_3\rangle, ..., |X_n\rangle$ as the input quantum states, and $|C_1\rangle, |C_2\rangle, |C_3\rangle, ..., |C_k\rangle$ as the centroids of the clusters $C_1, C_2, C_3, ..., C_k$.
2 Initial stage $|0\rangle|X_i\rangle|C_i\rangle$
3 Calculate distance from one data point (X_i) to centroid (C_i) using the formula, $\langle X_i|C_i\rangle = \langle 00|U_1U^\dagger|00\rangle = \sqrt{P_0}$
4 Assign cluster to the data point. Observe the nearest distance among $d^2(X_i, C_i)$ and perform superposition on data points. $|X_i\rangle \otimes |C_i\rangle|d^2(X_i, C_i)\rangle$
5 Perform Step 2 and Step 3 again until all the input quantum states are converged.

Suppose $|X\rangle = |X_1\rangle, \ldots |X_n\rangle$ are the datapoints encoded in the quantum states. k denotes the number of clusters and $|C\rangle = |C_1\rangle, \ldots, |C_k\rangle$ are the cluster centroids encoded in the quantum states. To minimize the cluster size within-cluster variance, $|W\rangle = |W_1\rangle, \ldots, |W_k\rangle$ is used.

Our improved hybrid classical-quantum (improved *qk*-means) approach uses the $UU^\dagger$ method (See Fig. 3 and algorithm steps in Algo. 1) to compute the distance between data points (input vector) and cluster centroids (centroids = 2), and then the data point is assigned to the nearest centroid. We note that the initial state is chosen to be $|0\rangle$ because, at the end of the algorithm, the probability of $|0\rangle$ is obtained, whose square root equals to the inner product of the centroid and test data. If the initial state is kept to $|1\rangle$, the probability of $|1\rangle$ needs to be measured, whose square root does not equal to the inner product. For example, $\langle 0|U^\dagger U|0\rangle = \langle 0|A|0\rangle = \sqrt{P_0}$, to achieve this, we need to first apply A on $|0\rangle$ state, then an arbitrary state can occur, $a|0\rangle + b|1\rangle$, in this case, if we measure P_0, its square root would be equal to a, which is $\langle 0|A|0\rangle$. However, if we prepare the initial state to be $|1\rangle$, and measure P_1, the square root of P_1, will not always be b, as b can contain some phase information, which P_1 cannot tell about. Here, we assume that a is always a real number because if it contains any phase information, it can be taken as common from both the terms and considered as the global phase. Similarly, this case can be scaled to any n-qubit system, where the initial state should be taken as $|0\rangle^{\otimes n}$. The improved *qk*-means algorithm updates the cluster centroid in the second step with the help of Eqs. (4) and (5).

$$\underset{D}{\operatorname{argmin}}(|X_i\rangle, |W_k\rangle) = \sum_{i=1}^{k} \sum_{x \epsilon W_i} d_2(|X_n\rangle, |W_k\rangle) \tag{4}$$

$$\underset{D}{\operatorname{argmin}}(|X_i\rangle, |C_k\rangle) = argmin \sum_{k=1}^{k} d_2(|X_n\rangle, |C_k\rangle) \tag{5}$$

3.4. LIME method for explainability

The clusters are created by using the improved qk-means clustering technique. Furthermore, LIME is used for the prediction explanation [55]. It is used to describe cluster formation and the grouping of breast and knee datasets. When different types of data are fed into improved *qk*-means model, the LIME explainer extracts the explanations and provides a local explanation for the predictions. It then performs tests and demonstrates what happens to the predictions.

Our proposed model learns some complex patterns as a combination of the selected features. It is difficult to summarize the whole decision boundary into one explanation. The basic idea of explanations with improved qk-means is to zoom into the local area of the individual predictions with the help of LIME (See Algo. 2). In the local region, simple explanations make sense, so the rest of the model gets a valid explanation for why the prediction is made. The designed interpretable models, i.e. integration of LIME and improved qk-means to get explanations, fits a linear interpretable model in the local area. It is a local approximation of a complex model. The complex models are complete black boxes, and the internals are hidden for LIME, so it is based on a model's inputs and outputs. In our experiment, the input is tabular data of images. Usually, domain experts in a specific field have some prior knowledge about the problem. In the paper, we provide explanations to improve the acceptance of a predictive algorithm. For LIME, the requirement is that the explanations are locally faithful, but at the same time, explanations might not make sense globally. Hence, throughout this paper, the experiment focuses on the local area around the output predictions.

$$X = \underset{g \epsilon G}{\operatorname{argmin}} L(f, g, \pi_x) + \omega(g) \tag{6}$$

$$L(f, g, \pi_x) = \sum_{Z} \pi_x(z)(f(z) - g(z'))^2 \tag{7}$$

Now consider Eq. (7) for the mathematical optimization problem used in LIME. For instance, knowing the properties of breast cancer and MRI data in the tabular format which is the input data point X. In the optimization formula in [56], the complex model is denoted by f, and the linear model is denoted by g, which comes from the set of interpretable models, denoted by G (G is the family of a linear model). The loss function in optimization means looking for an approximation of the complex model f by the simple model g in the neighborhood of data point X (good approximation from a neighbor). The third argument π defines local neighborhoods of the selected data points and is some proximity measure. The final term is to regularize the complexity of the simple surrogate model. For the improved qk-means algorithm, a desirable condition could be to have many zero-weighted input features, which makes the explanation simpler when ignoring most of the features. Overall, ω is a complexity measure, and an optimization is a minimization problem, i.e., minimizing the complexity. The loss function says that the g argument in the *argmin* minimizes those two loss terms, so it should be an approximate complex model in that local area and stays as simple as possible. By achieving the good clustering accuracy, The complex model f and all input feature values minimizes the loss term. $f(z)$ is the label which comes from the imrpoved *qk*-means model and z' is the prediction model. The loss function, used for optimizing a model, is the sum of square distances between $f(z)$ and z'.

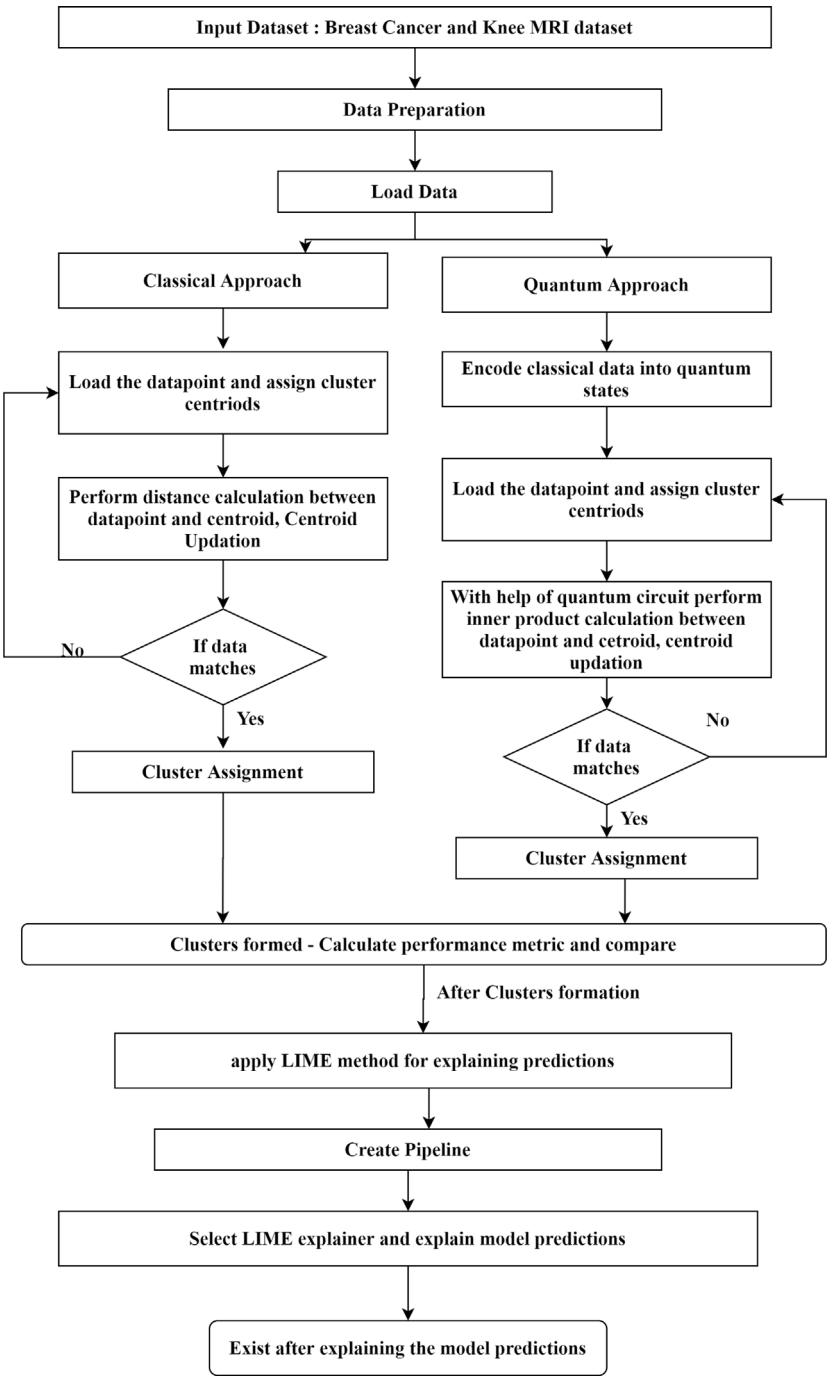

Fig. 4. The process flow of the hybrid approach using the quantum clustering of the labeling of the datasets and the LIME method to explain the prediction given by the improved *qk*-means clustering algorithm.

Fig. 4 illustrates the flow of the improved *qk*-means approach and classical approach for explaining the predictions. Therefore, the results from both approaches explain using the local explainer and provide the description of the prediction.

4. Experimental result

4.1. Evaluation environment and metric

The IBM quantum environment provides high-performance simulators for simulating various algorithms and quantum circuits under actual noise models. Experiments are performed on IBM quantum simulators, i.e. qasm simulator, which is based on superconducting transmon qubits to export measurement count. We have used the three-qubit quantum circuits to perform distance calculations and the centroid updation to maintain the cluster quality. Fig. 3 illustrates the quantum circuit used to show the improved *qk*-means algorithm evaluation.

The evaluation metric can be found as follows:

$$\text{Accuracy} = \sum_{X=x_i,..,x_n}^{c} = \frac{TP_X + TN_X}{TP_X + TN_X + FP_X + FN_X} \tag{8}$$

$$\text{Precision} = \sum_{X=x_i,..,x_n}^{c} = \frac{TP_X}{TP_X + FN_X} \tag{9}$$

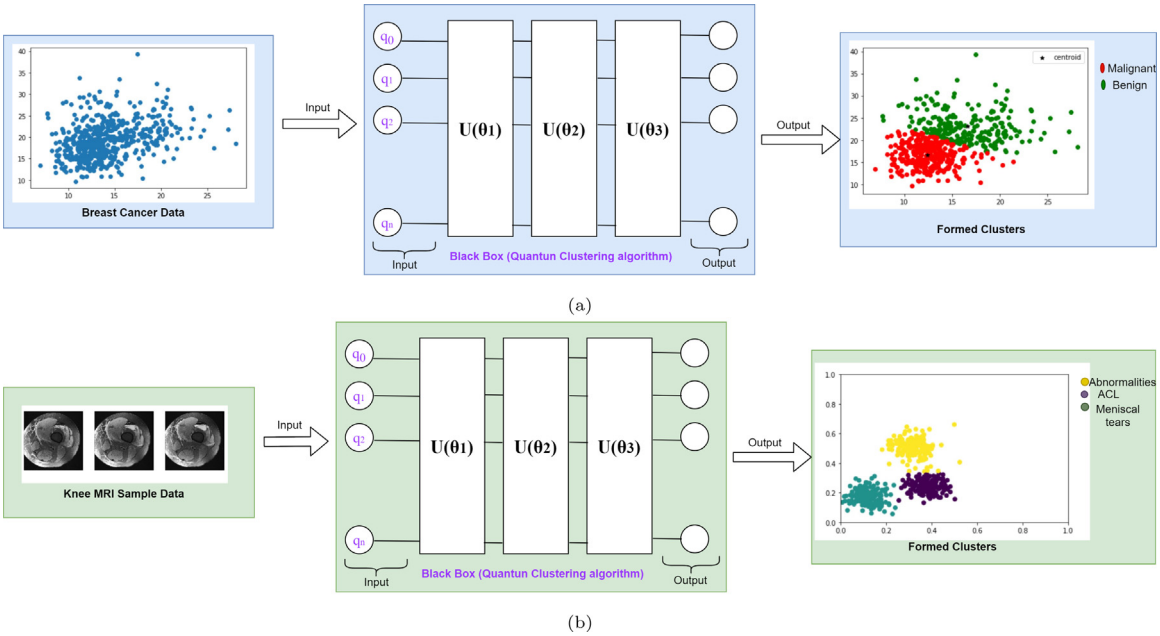

Fig. 5. (a) The clustering results given by the qk-means algorithm using the features of the Breast Cancer dataset. The scatter plot shows the two clusters representing benign and Malignancy. (b) The illustration shows that the three types of Knee series result from the quantum clustering algorithm. The predicted results form three clusters for ACL, meniscal tears, and abnormalities.

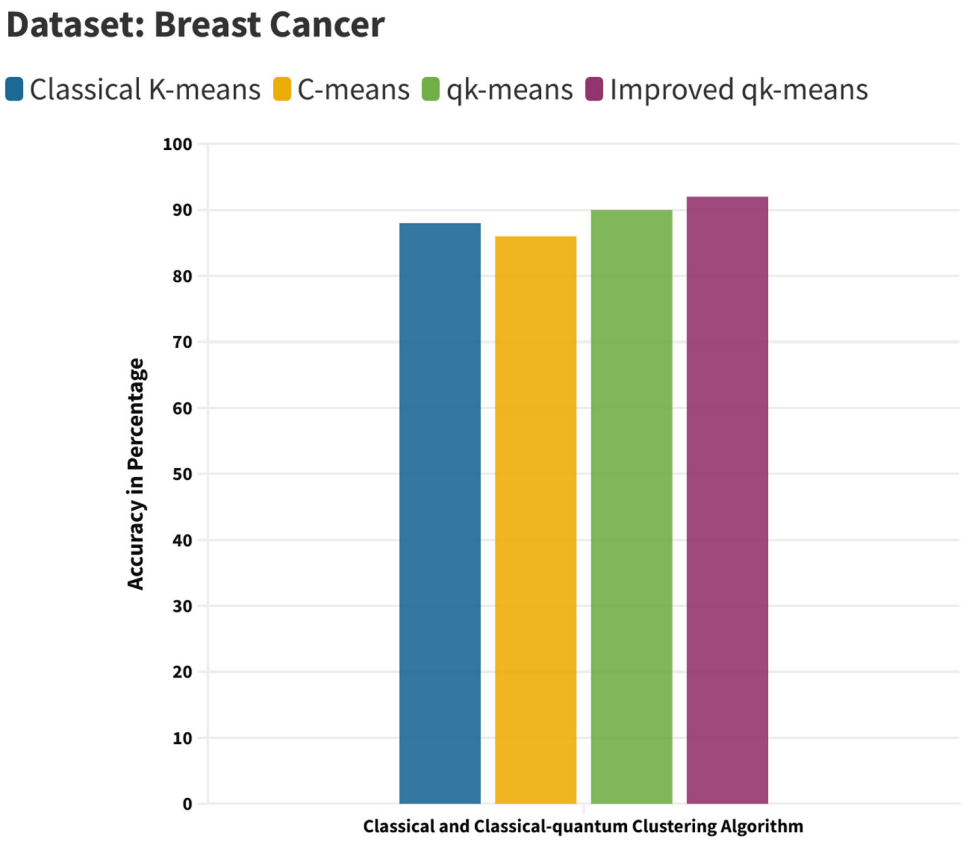

Fig. 6. Using the breast cancer dataset, the bar graph compares the accuracy of classical clustering algorithms like K-means and C-means and classical-quantum clustering algorithms like qk-means and our improved qk-means algorithm.

$$\text{Recall} = \sum_{X=x_i,\ldots,x_n}^{C} = \frac{TP_X + TN_X}{TP_X + FP_X} \tag{10}$$

$$TP_{X_i} = \sum_{i=1}^{n} X_n \tag{11}$$

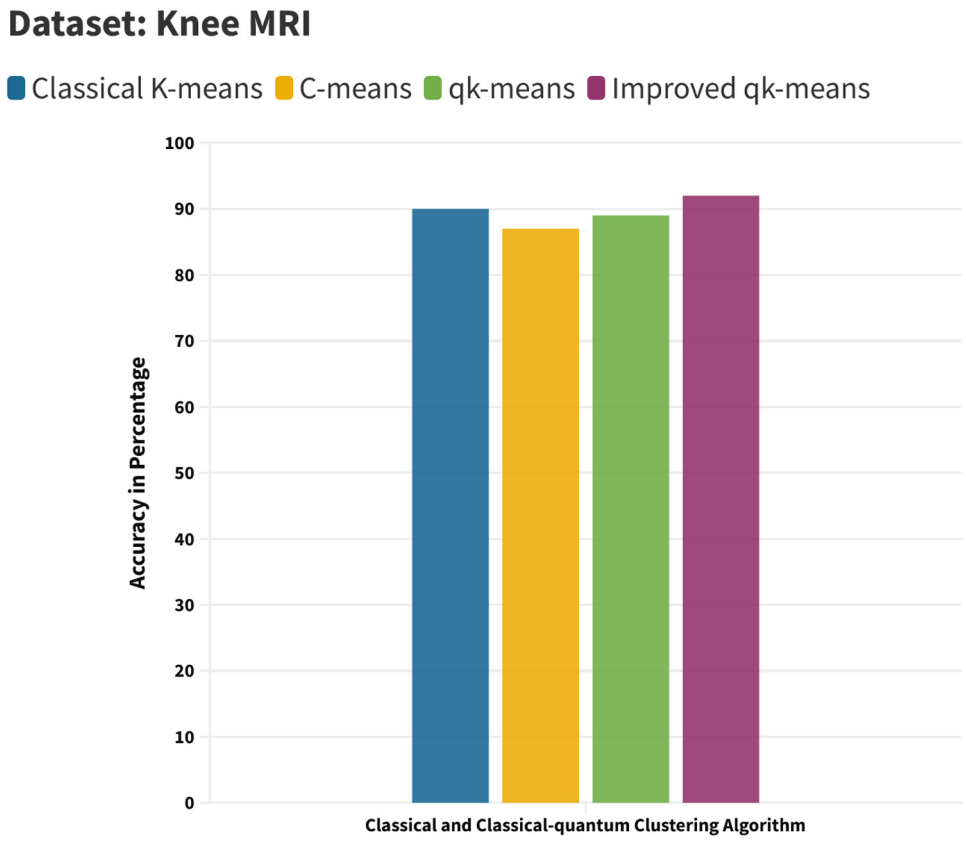

Fig. 7. The accuracy of the classical-quantum clustering methods, such as qk-means and our improved qk-means algorithm, and traditional classical clustering algorithms, such as K-means and C-means, using the Knee MRI dataset is presented in the bar graph.

Algorithm 2: Hybrid approach of LIME and Improved *qk*-means algorithm to explain the features

Input Classical data
Output Prediction and explanations of the data
1 Test data
2 Estimate distance between test data points and centroids
3 Make clusters and predictions on new data using the improved *qk*-means algorithm
4 Choose n number of features that best describes the quantum clustering model predictions from the test data.
5 Feature weights from the simple model make explanations for the model's local behavior.

$$TN_{X_i} = \sum_{j=1}^{c}\sum_{k=1}^{c} X_j k, j \neq i, k \neq i \tag{12}$$

$$FP_{X_i} = \sum_{j=1}^{c} X_j i, j \neq i \tag{13}$$

$$FN_{X_i} = \sum_{i=1}^{c} X_i j, j \neq i \tag{14}$$

$$Accuracy(C, C') = max_{perm \epsilon p} \frac{1}{n} \sum_{i=0}^{n-1} 1(perm(C_i') = C_i) \tag{15}$$

$$S = \sum_{i=0} \frac{b_i - a_i}{max(a_i * b_i)} \tag{16}$$

4.2. Quantitative and visualization results

We form the learning task by taking the image data, especially paper focused on a digitized image of a fine needle aspirate (FNA) of a breast mass (UCI repository). First, we train the model and then we use the learning model to produce two clusters as the following:

- Cluster of a malignancy
- Cluster of a benign

In our dataset, there is multicollinearity as the features (such as radius mean, area mean and parameter mean) depend on each other and affect the model's performance (See Fig. 5(a)). So we chose area mean as one of the features for calculating clusters. Furthermore, there are two independent features such as concavity and compactness, for which regression method can be used for the feature selection.

Both input datasets are clustered and classified using a variety of algorithms. Tables 2 and 3 show the existing ML algorithms, *qk*-means algorithm and improved *qk*-means algorithm. First, the classical clustering algorithms, which include the K-means [52], and C-means [53] are used. The classification methods, i.e. KNN [34,35], Random Forest [36], SVM [37], and Logistic regression [38], are then used to demonstrate comparison and locate gaps to discover any hidden patterns in the data. The evaluation metrics like precision, recall, and F-measures are used to measure the performance of classification methods. After discussing the results of classical clustering and classification methods, we employed the *qk*-means algorithm, and improved *qk*-means algorithm. We may infer from Table 3 that the clustering accuracy obtained from our improved qk-means algorithm is

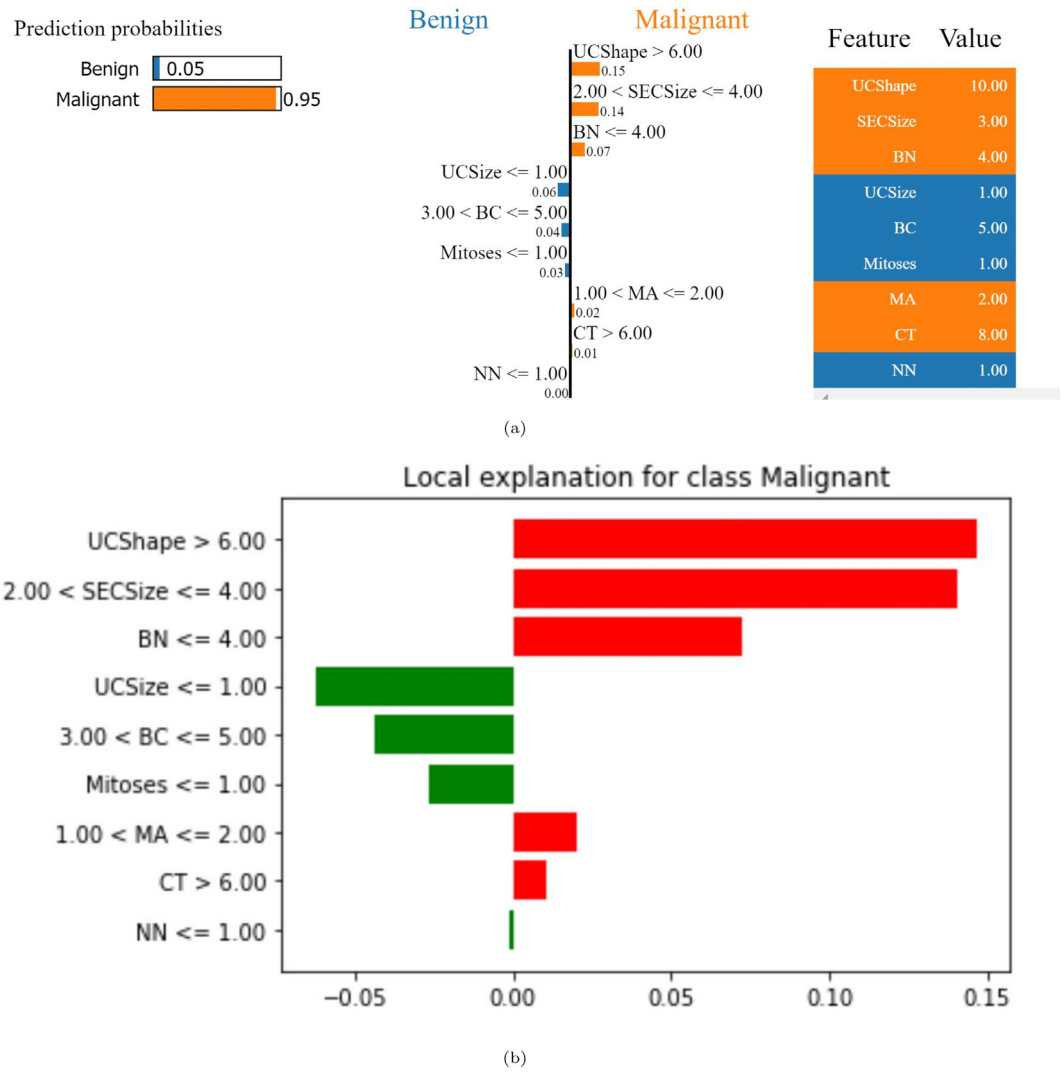

Fig. 8. (a) The illustration shows the relation between the corresponding feature and predictions of Malignant. The orange color shows the positively correlated features. (b) The illustration shows the local explanation for Malignant. The green-colored feature shows the negatively correlated features.

better for clustering the input data. We modified the classical k-means algorithm's assignment stage to choose a random centroid from those near the closest centroid to implement our improved qk-means algorithm, and we added errors to updated clusters. The completeness and accuracy of the evaluation are two criteria used for the classical and classical-quantum clustering algorithms (See Eqs. (15) and (16)). A clustering is fully complete when each cluster contains information pointing to other clusters that are similar to it. The completeness metric shows how closely the clustering technique adheres to the ideal (completeness score). A permutation of the cluster label values does not alter the score value. Knowledge of the actual labels of the data points is optional to understand the silhouette coefficient. Only the initial, unlabeled sample and the clustering outcome are used to measure the clustering's quality. To begin, the silhouette score is calculated for each observation. Let p be the average distance between the data points from the closest cluster, and d represents the mean distance between data points inside a cluster (different from the one datapoint belongs to). The silhouette measure is then presented in Eq. (16). The outcomes of clustering will be better if the silhouette score (S) is higher. By calculating the number of clusters that maximizes the silhouette coefficient, the silhouette score is used to determine the ideal number of clusters k. Our improved qk-means clustering algorithm updates the centroids after the cluster assignment. It helps to form the quality cluster while new data points are added to the new clusters. For each model, functions need to be created that follow a similar structure, executing all algorithms and setting random states to zero. The KNN and random forest model set the criterion equal to entropy which is used to calculate the information gain within the data points of the model [34,36]. Both the train and test data are passed through the algorithms to check the classification accuracy as shown in Table 2. The random forest and KNN performed with the classification accuracies of 90.1% and 88.7% respectively. Then the quality of the predictions are made and calculated using the true and false positives and negatives. The possible outcomes of the binary classification are TP: True Positive, TN: True Negative, FP: False Positive, FN: False Negative. The input data is clustered into c classes. Table 2 discusses the model's classification accuracy metric, i.e., precision and recall from Eq. (8) to Eq. (14). The comparison between the existing qk-means method and our improved qk-means algorithm is shown in Table 3 and Fig. 6. Utilizing the completeness, silhouette score, and accuracy, the revised qk-means algorithm's prediction and cluster quality are assessed. With clustering accuracies of 92.6% and 93.7% respectively, our improved qk-means algorithm is used to explain the predictions from the breast cancer and knee MRI data (See Figs. 6 and 7). The trust determining in prediction is

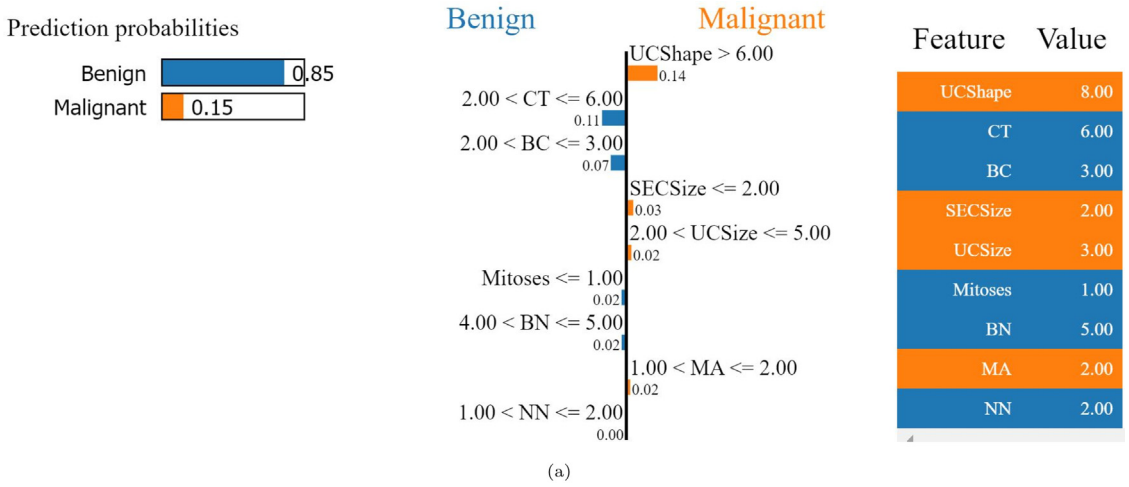

(a)

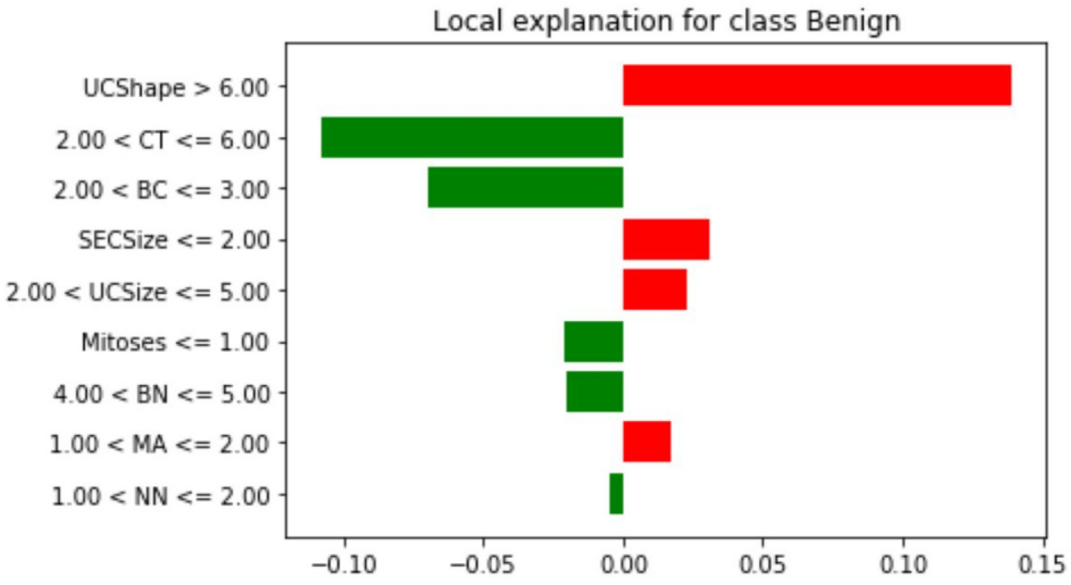

(b)

Fig. 9. (a) The illustration shows the relation between the corresponding feature and predictions of Benign. The orange color shows the positively correlated features, and the blue color features show the negatively correlated features against Malignant. (b) The illustration shows the local explanation for Benign. The green-colored feature shows the negatively correlated features against the prediction results of Malignant.

essential to making decisions using the improved *qk*-means. After assessing the effective outcomes from our modified qk-means, we provide a local explanation for the created clusters.

5. Discussion

The medical data has more dimensions and relationships between predictors and outcome variables. The complex relationship makes it challenging to build a model that provides information about all the detailed information or relations. The feature importance plot is one of the solutions to find essential features while predicting the outcome. However, it does not give the indication or direction of the mapping between the features. In the experiment, seven features of a breast cancer dataset and five features of a Knee MRI dataset are used. First, the decision boundary of a model needs to be measured and checked whether the data point is Benign or Malignant. So the prediction made is highly non-linear (there is no easy way to explain the relationship in how we perform predictions). LIME showcases the features to create or develop predictions when we have many features available. We use LIME with the improved qk-means algorithm to develop the predictions from the breast cancer dataset (Algo. 2 and Fig. 4). LIME takes the observations and calculates the distance metrics or similarities between the test dataset. The improved qk-means algorithm makes clusters for predictors. Finally, LIME tries a combination of predictors, i.e. *n* number of predictors, to figure out the minimum number of predictors that gives the maximum likelihood of the clusters predicted by the improved qk-means algorithm. It picks *n* features with similarity scares to derive coefficients, which serves as an explanation for the local scale's observation. LIME gets a pipeline that begins with data pre-processing and runs the ML model (here, we used improved *qk*-means algorithm) as input for interpreting the model result. The LIME method offers various categories of the model for various data types such as tabular, image, text, etc. In our paper, tabular data is used, so the tabular explainer is selected to explain the predictions ("LimeTabularExplainer"). Once the improved *qk*-means model has been trained, the LIME explainer gives the relation between the selected feature and prediction. Figs. 8 and 9 illustrate the prediction of malignant and benign, respectively. The top left corner of Figs. 8(a) and 8(b) illustrate the prediction

and details of positively and negatively correlated features. The prediction of benign provides positive and negative correlations to the prediction of malignant. In both Figs. 8 and 9, the green color shows a negative relation against the result of malignant. The green color depicts the negative relation against the result of malignant but benign results favor.

6. Conclusion

In this paper, we implement improved qk-means clustering algorithm, and test them on the Breast Cancer and Knee MRI datasets. We then calculate, compare, and evaluate the various results based on accuracy, completeness, and silhouette score to demonstrate the clustering accuracy and reliability of the improved qk-means algorithm. Following a precise comparison of our models, we show that our proposed improved qk-means clustering algorithm outperforms all exisitng algorithms with a greater accuracy of 93.2% and completeness of 94.5%. We merge the LIME approach and the improved qk-means clustering algorithm to explain the predictions. XAI models pose complex challenges and offer various opportunities for the medical sector. Recent research and proposed methods show promising directions and provide solutions using quantum explainability to model medical data.

XAI accelerates decision speed by achieving transparency in solving complex problems. The classical machine is reaching its limit, so we need explainable quantum models to learn from hidden patterns in medical data. Quantum computing has demonstrated exciting potential to accelerate ML and data science-related applications and so on in the future.

CRediT authorship contribution statement

Shradha Deshmukh: Literature analysis, Interpretation of results and the preparation of the manuscript. **Bikash K. Behera:** Literature analysis, Interpretation of results and the preparation of the manuscript. **Preeti Mulay:** Literature analysis, Interpretation of results and the preparation of the manuscript. **Emad A. Ahmed:** Literature analysis, Interpretation of results and the preparation of the manuscript. **Saif Al-Kuwari:** Literature analysis, Interpretation of results and the preparation of the manuscript. **Prayag Tiwari:** Literature analysis, Interpretation of results and the preparation of the manuscript. **Ahmed Farouk:** Literature analysis, Interpretation of results and the preparation of the manuscript.

Declaration of competing interest

The authors declare that they have no known competing financial interests or personal relationships that could have appeared to influence the work reported in this paper.

Data availability

The source code of the described method is available on GitHub (https://github.com/shradha-deshmukh/Explainable-Quantum-Clustering.git).

References

[1] A.J. London, Artificial intelligence and black-box medical decisions: accuracy versus explainability, Hastings Cent. Rep. 49 (1) (2019) 15–21.

[2] D. Slack, A. Hilgard, S. Singh, H. Lakkaraju, Reliable post hoc explanations: Modeling uncertainty in explainability, Adv. Neural Inf. Process. Syst. 34 (2021) 9391–9404.

[3] I.P. de Sousa, M.M.B.R. Vellasco, E.C. da Silva, Explainable artificial intelligence for bias detection in covid ct-scan classifiers, Sensors 21 (16) (2021) 5657, http://dx.doi.org/10.3390/s21165657.

[4] S. Vollert, M. Atzmueller, A. Theissler, Interpretable machine learning: A brief survey from the predictive maintenance perspective, in: 2021 26th IEEE International Conference on Emerging Technologies and Factory Automation, ETFA, IEEE, 2021, pp. 01–08.

[5] E. Tjoa, C. Guan, A survey on explainable artificial intelligence (xai): Toward medical xai, IEEE Trans. Neural Netw. Learn. Syst. 32 (11) (2020) 4793–4813.

[6] N. Bussmann, P. Giudici, D. Marinelli, J. Papenbrock, Explainable AI in fintech risk management, Front. Artif. Intell. 3 (2020) 26.

[7] J. Lötsch, D. Kringel, A. Ultsch, Explainable artificial intelligence (XAI) in biomedicine: Making AI decisions trustworthy for physicians and patients, BioMedInformatics 2 (1) (2022) 1–17.

[8] H.W. Loh, C.P. Ooi, S. Seoni, P.D. Barua, F. Molinari, U.R. Acharya, Application of explainable artificial intelligence for healthcare: A systematic review of the last decade, Comput. Methods Programs Biomed. (2022) 107161.

[9] Y.-L. Chou, C. Moreira, P. Bruza, C. Ouyang, J. Jorge, Counterfactuals and causability in explainable artificial intelligence: Theory, algorithms, and applications, Inf. Fusion 81 (2022) 59–83, http://dx.doi.org/10.1016/j.inffus.2021.11.003.

[10] S.R. Islam, W. Eberle, S.K. Ghafoor, M. Ahmed, Explainable artificial intelligence approaches: A survey, 2021, arXiv preprint arXiv:2101.09429.

[11] M. Erwig, P. Kumar, Explainable dynamic programming, J. Funct. Programming 31 (2021) http://dx.doi.org/10.1017/S0956796821000083.

[12] A. Kalantari, A. Kamsin, S. Shamshirband, A. Gani, H. Alinejad-Rokny, A.T. Chronopoulos, Computational intelligence approaches for classification of medical data: State-of-the-art, future challenges and research directions, Neurocomputing 276 (2018) 2–22, http://dx.doi.org/10.1016/j.neucom.2017.01.126.

[13] I. Scholl, T. Aach, T.M. Deserno, T. Kuhlen, Challenges of medical image processing, Comput. Sci. Res. Dev. 26 (1) (2011) 5–13, http://dx.doi.org/10.1007/s00450-010-0146-9.

[14] A. Ampavathi, Research challenges and future directions towards medical data processing, Comput. Methods Biomech. Biomed. Eng. Imaging Visual. (2022) 1–20.

[15] Y. Zhang, Y. Weng, J. Lund, Applications of explainable artificial intelligence in diagnosis and surgery, Diagnostics 12 (2) (2022) 237, http://dx.doi.org/10.3390/diagnostics12020237.

[16] M.S. Kamal, N. Dey, L. Chowdhury, S.I. Hasan, K. Santosh, Explainable AI for glaucoma prediction analysis to understand risk factors in treatment planning, IEEE Trans. Instrum. Meas. 71 (2022) 1–9, http://dx.doi.org/10.1109/TIM.2022.3171613, URL https://doi.org/10.1109/TIM.2022.3171613.

[17] A.B. Arrieta, N. Díaz-Rodríguez, J. Del Ser, A. Bennetot, S. Tabik, A. Barbado, S. García, S. Gil-López, D. Molina, R. Benjamins, et al., Explainable artificial intelligence (XAI): Concepts, taxonomies, opportunities and challenges toward responsible AI, Inf. Fusion 58 (2020) 82–115.

[18] S. Mohseni, N. Zarei, E.D. Ragan, A multidisciplinary survey and framework for design and evaluation of explainable AI systems, ACM Trans. Interact. Intell. Syst. (TiiS) 11 (3–4) (2021) 1–45.

[19] H. Bansal, B. Chinagundi, P.S. Rana, N. Kumar, An ensemble machine learning technique for detection of abnormalities in knee movement sustainability, Sustainability 14 (20) (2022) 13464, http://dx.doi.org/10.3390/su142013464.

[20] Q. Liu, L. Wang, T-test and ANOVA for data with ceiling and/or floor effects, Behav. Res. Methods 53 (1) (2021) 264–277, http://dx.doi.org/10.3758/s13428-020-01407-2.

[21] D. Kim, J. Chung, J. Choi, M.D. Succi, J. Conklin, M.G.F. Longo, J.B. Ackman, B.P. Little, M. Petranovic, M.K. Kalra, et al., Accurate auto-labeling of chest X-ray images based on quantitative similarity to an explainable AI model, Nature Commun. 13 (1) (2022) 1–15, http://dx.doi.org/10.1038/s41467-022-29437-8.

[22] S. Panakkal, B. Falkenstein, A.B. Tosun, B. Campbell, M. Becich, J. Fine, D.L. Taylor, S.C. Chennubhotla, F. Pullara, TumorMapr™ analytical software platform: Unbiased spatial analytics and explainable AI (xAI) platform for generating data, extracting information, and creating knowledge from multi to hyperplexed fluorescence and/or mass spectrometry image datasets, Cancer Res. 82 (12_Supplement) (2022) 454, http://dx.doi.org/10.1158/1538-7445.AM2022-454.

[23] M. Hossain, S.S. Haque, H. Ahmed, H.A. Mahdi, A. Aich, Early stage detection and classification of colon cancer using deep learning and explainable AI on histopathological images (Ph.D. thesis), Brac University, 2022.

[24] N. Gozzi, E. Giacomello, M. Sollini, M. Kirienko, A. Ammirabile, P. Lanzi, D. Loiacono, A. Chiti, Image embeddings extracted from CNNs outperform other transfer learning approaches in chest radiographs' classification, Diagnostics (2022) http://dx.doi.org/10.21203/rs.3.rs-1361817/v1.

[25] W.H. Abir, M. Uddin, F.R. Khanam, T. Tazin, M.M. Khan, M. Masud, S. Aljahdali, et al., Explainable AI in diagnosing and anticipating leukemia using transfer learning method, Comput. Intell. Neurosci. 2022 (2022) http://dx.doi.org/10.1155/2022/5140148.

[26] P. Silitonga, Clustering of patient disease data by using K-means clustering, Int. J. Comput. Sci. Inform. Secur. (IJCSIS) 15 (7) (2017) 219–221.

[27] J. Biamonte, P. Wittek, N. Pancotti, P. Rebentrost, N. Wiebe, S. Lloyd, Quantum machine learning, Nature 549 (7671) (2017) 195–202, http://dx.doi.org/10.1038/nature23474.
[28] P. Tiwari, S. Dehdashti, A.K. Obeid, P. Marttinen, P. Bruza, Kernel method based on non-linear coherent states in quantum feature space, J. Phys. A 55 (35) (2022) 355301.
[29] N. Laxminarayana, N. Mishra, P. Tiwari, S. Garg, B.K. Behera, A. Farouk, Quantum-assisted activation for supervised learning in healthcare-based intrusion detection systems, IEEE Trans. Artif. Intell. (2022) 1–8, http://dx.doi.org/10.1109/TAI.2022.3187676, URL https://ieeexplore.ieee.org/document/9813378.
[30] S. Moradi, C. Brandner, C. Spielvogel, D. Krajnc, S. Hillmich, R. Wille, W. Drexler, L. Papp, Clinical data classification with noisy intermediate scale quantum computers, Sci. Rep. 12 (1) (2022) 1–9, http://dx.doi.org/10.1038/s41598-022-05971-9.
[31] M. Kapcia, H. Eshkiki, J. Duell, X. Fan, S. Zhou, B. Mora, ExMed: An AI tool for experimenting explainable AI techniques on medical data analytics, in: 2021 IEEE 33rd International Conference on Tools with Artificial Intelligence, ICTAI, IEEE, 2021, pp. 841–845, http://dx.doi.org/10.1109/ICTAI52525.2021.00134.
[32] H. Yoo, S. Han, K. Chung, Diagnosis support model of cardiomegaly based on CNN using ResNet and explainable feature map, IEEE Access 9 (2021) 55802–55813, http://dx.doi.org/10.1109/ACCESS.2021.3068597.
[33] S. Knapič, A. Malhi, R. Saluja, K. Främling, Explainable artificial intelligence for human decision support system in the medical domain, Mach. Learn. Knowl. Extract. 3 (3) (2021) 740–770, http://dx.doi.org/10.3390/make3030037.
[34] J.-B. Lamy, B. Sekar, G. Guezennec, J. Bouaud, B. Séroussi, Explainable artificial intelligence for breast cancer: A visual case-based reasoning approach, Artif. Intell. Med. 94 (2019) 42–53, http://dx.doi.org/10.1016/j.artmed.2019.01.001.
[35] T.A. Assegie, An optimized K-nearest neighbor based breast cancer detection, J. Robot. Control (JRC) 2 (3) (2021) 115–118, http://dx.doi.org/10.18196/jrc.2363.
[36] B. Dai, R.-C. Chen, S.-Z. Zhu, W.-W. Zhang, Using random forest algorithm for breast cancer diagnosis, in: 2018 International Symposium on Computer, Consumer and Control (IS3C), IEEE, 2018, pp. 449–452, http://dx.doi.org/10.1109/IS3C.2018.00119.
[37] S. Vashisth, I. Dhall, G. Aggarwal, Design and analysis of quantum powered support vector machines for malignant breast cancer diagnosis, J. Intell. Syst. 30 (1) (2021) 998–1013.
[38] R.C. Ripan, I.H. Sarker, S.M. Hossain, M. Anwar, R. Nowrozy, M.M. Hoque, M. Furhad, et al., A data-driven heart disease prediction model through K-means clustering-based anomaly detection, SN Comput. Sci. 2 (2) (2021) 1–12, http://dx.doi.org/10.1007/s42979-021-00518-7.
[39] J.M. Clementino, B.S. Faiçal, C.C. Bones, C. Traina, M.A. Gutierrez, A.J. Traina, Multilevel clustering explainer: An explainable approach to electronic health records, in: 2021 IEEE 34th International Symposium on Computer-Based Medical Systems, CBMS, IEEE, 2021, pp. 253–258, http://dx.doi.org/10.1109/CBMS52027.2021.00073.
[40] M.S. Kamal, N. Dey, L. Chowdhury, S.I. Hasan, K. Santosh, Explainable AI for glaucoma prediction analysis to understand risk factors in treatment planning, IEEE Trans. Instrum. Meas. 71 (2022) 1–9, http://dx.doi.org/10.1109/TIM.2022.3171613.
[41] D. Yeboah, L. Steinmeister, D.B. Hier, B. Hadi, D.C. Wunsch, G.R. Olbricht, T. Obafemi-Ajayi, An explainable and statistically validated ensemble clustering model applied to the identification of traumatic brain injury subgroups, IEEE Access 8 (2020) 180690–180705, http://dx.doi.org/10.1109/ACCESS.2020.3027453.
[42] H. Han, W. Li, J. Wang, G. Qin, X. Qin, Enhance explainability of manifold learning, Neurocomputing (2022) http://dx.doi.org/10.1016/j.neucom.2022.05.119.
[43] Kaggle: Your Machine Learning and Data Science Community, URL https://www.kaggle.com.
[44] B. Zheng, S.W. Yoon, S.S. Lam, Breast cancer diagnosis based on feature extraction using a hybrid of K-means and support vector machine algorithms, Expert Syst. Appl. 41 (4) (2014) 1476–1482, http://dx.doi.org/10.1016/j.eswa.2013.08.044.
[45] K.C. Gowda, E. Diday, Symbolic clustering using a new dissimilarity measure, Pattern Recognit. 24 (6) (1991) 567–578, http://dx.doi.org/10.1016/0031-3203(91)90022-W.
[46] K.M. Boehm, P. Khosravi, R. Vanguri, J. Gao, S.P. Shah, Harnessing multimodal data integration to advance precision oncology, Nat. Rev. Cancer 22 (2) (2022) 114–126, http://dx.doi.org/10.1038/s41568-021-00408-3.
[47] T.Y. Wen, S.A.M. Aris, Hybrid approach of EEG stress level classification using K-means clustering and support vector machine, IEEE Access 10 (2022) 18370–18379, http://dx.doi.org/10.1109/ACCESS.2022.3148380.
[48] R. Tripathy, R.K. Nayak, Eukaryotic plasma cholesterol prediction from human GPCRs using K-means with support vector machine, in: Advanced Deep Learning for Engineers and Scientists, Springer, 2021, pp. 243–257, http://dx.doi.org/10.1007/978-3-030-66519-7_10.
[49] M. Schuld, N. Killoran, Quantum machine learning in feature Hilbert spaces, Phys. Rev. Lett. 122 (4) (2019) 040504, http://dx.doi.org/10.1103/PhysRevLett.122.040504.
[50] A.Y. Wei, P. Naik, A.W. Harrow, J. Thaler, Quantum algorithms for jet clustering, Phys. Rev. D 101 (9) (2020) 094015.
[51] A.W. Harrow, Small quantum computers and large classical data sets, 2020, arXiv preprint arXiv:2004.00026.
[52] Z. Huang, Extensions to the k-means algorithm for clustering large data sets with categorical values, Data Min. Knowl. Discov. 2 (3) (1998) 283–304, http://dx.doi.org/10.1023/A:1009769707641.
[53] B.R. Reddy, Y.V. Kumar, M. Prabhakar, Clustering large amounts of healthcare datasets using fuzzy c-means algorithm, in: 2019 5th International Conference on Advanced Computing & Communication Systems, ICACCS, IEEE, 2019, pp. 93–97, http://dx.doi.org/10.1109/ICACCS.2019.8728503.
[54] S.U. Khan, A.J. Awan, G. Vall-Llosera, K-means clustering on noisy intermediate scale quantum computers, 2019, arXiv preprint arXiv:1909.12183.
[55] X.-H. Li, C.C. Cao, Y. Shi, W. Bai, H. Gao, L. Qiu, C. Wang, Y. Gao, S. Zhang, X. Xue, et al., A survey of data-driven and knowledge-aware explainable ai, IEEE Trans. Knowl. Data Eng. 34 (1) (2020) 29–49, http://dx.doi.org/10.1109/TKDE.2020.2983930.
[56] A. Holzinger, A. Saranti, C. Molnar, P. Biecek, W. Samek, Explainable AI methods-a brief overview, in: International Workshop on Extending Explainable AI beyond Deep Models and Classifiers, Springer, 2022, pp. 13–38, http://dx.doi.org/10.1007/978-3-031-04083-2_2.